Altered prefrontal signaling during inhibitory control in a salient drug context in human cocaine addiction

Abbreviated title: Salience and control interaction in CUD via fMRI

Ahmet O. Ceceli, Ph.D.* [1], Muhammad A. Parvaz, Ph.D.* [1,2], Sarah King [2], Matthew Schafer [2], Pias Malaker [1], Akarsh Sharma [1], Nelly Alia-Klein, Ph.D. [1,2], & Rita Z. Goldstein, Ph.D. [1,2]

[1] Department of Psychiatry, Icahn School of Medicine at Mount Sinai, 1 Gustave L. Levy Place, Box 1230, New York, NY 10029

[2] Department of Neuroscience, Friedman Brain Institute, Icahn School of Medicine at Mount Sinai, 1 Gustave L. Levy Place, Box 1065, New York, NY 10029

* Equal contribution

Corresponding author: Rita Z. Goldstein (rita.goldstein@mssm.edu)

Number of pages: 21

Number of figures: 5

Number of tables: 4

Number of words in Abstract: 202, Introduction: 644, Discussion: 1497

Conflict of interest statement: The authors declare no competing financial interests.

Acknowledgements: This work was supported by F32DA033088 and K01DA043615 to MAP, 1R01DA041528, R01DA023579, and R21DA034954 to RZG.

Abstract

Drug addiction is characterized by impaired Response Inhibition and Salience Attribution (iRISA), where the salience of drug cues is postulated to overpower that of other reinforcers with a concomitant decrease in self-control. However, the neural underpinnings of the interaction between the salience of drug cues and inhibitory control in drug addiction remain unclear. We developed a novel stop-signal fMRI task where the stop-signal reaction time (SSRT—a classical inhibitory control measure) was tested under different salience conditions (modulated by drug, food, threat or neutral words) in individuals with cocaine use disorder (CUD; n=26) vs. demographically matched healthy control participants (HC; n=26). Despite similarities in drug cue-related SSRT and valence and arousal word ratings between groups, the dorsolateral prefrontal cortex (dlPFC) activity was diminished during the successful inhibition of drug versus food cues in CUD, and was correlated with lower frequency of recent use, lower craving, and longer abstinence ($Z > 3.1$, $p < .05$ corrected). Results suggest reduced involvement of cognitive control regions (e.g., dlPFC) during inhibitory control under a drug context, relative to an alternative reinforcer, in CUD. Supporting the iRISA model, these results elucidate the direct impact of drug-related cue-reactivity on the neural signature of inhibitory control in drug addiction.

Significance statement

Excessive salience attribution to drugs and related cues at the expense of nondrug reinforcers and cues and inhibitory control impairments are hallmark symptoms of drug addiction. Although these neuropsychological functions have been investigated independently, brain representations of their interaction are less clear. We illustrate that, despite matched behavioral performance and valence and arousal ratings, the dorsolateral prefrontal cortex—a key node of the cognitive control network also associated with craving—exhibits decreased signaling when successfully inhibiting responses to drug compared to nondrug (food) cues (words) in cocaine-addicted individuals. Modulating salience while

taxing self-control permits the study of their combined impact, an ecologically valid examination of the addiction experience. Better understanding inhibitory control under drug cue-reactivity may refine targeted neuromodulatory interventions.

Introduction

The impaired response inhibition and salience attribution (iRISA) model of drug addiction posits that addicted individuals attribute excessive salience to drug and drug-related cues at the expense of non-drug-related reinforcers, with concomitant decreases in inhibitory control (Goldstein and Volkow, 2002, 2011). Consistent with the animal literature (Phillips et al., 2003), in human neuroimaging studies increased responses in the mesencephalon (Goldstein et al., 2009b), anterior cingulate cortex and ventromedial prefrontal cortex (vmPFC; Kober et al., 2016; Konova et al., 2019), and connectivity between salience, reward, and executive networks (Ray et al., 2015), have been interpreted to reflect the excessive salience attributed to drug cues in drug-addicted individuals. Inhibitory control (in non-drug contexts) has instead been associated with hypoactivations in the inferior frontal gyrus (IFG), orbitofrontal cortex (OFC), and dorsolateral PFC (dlPFC) in this population as previously reviewed (Zilverstand et al., 2018; Ceceli et al., 2021). However, the interaction between inhibitory control and drug cue reactivity, crucial for more accurately examining the neurobehavioral bases of drug addiction's core phenomenology, has yet to be well-characterized.

Several neuroimaging studies in addicted individuals have used drug related vs. non-drug related cues in the context of tasks approximating inhibitory control such as the Go/No-Go (Ames et al., 2014; Czapla et al., 2017; Gilman et al., 2018) and Stroop tasks (Carpenter et al., 2006; Hester et al., 2006; Goldstein et al., 2007, 2009b, 2009a; Smith and Ersche, 2014; DeVito et al., 2018). Using the Go/No-Go task, increased activations in the dlPFC, vmPFC, and insula during alcohol-related No-Go vs. non-alcohol Go trials have been reported in alcohol dependent subjects (Ames et al., 2014; Czapla et al., 2017) [with negative results in smokers (Gilman et al., 2018)]. Instead of measuring the classical Stroop conflict induced by reading (faster) vs. naming (slower) of incongruent color words (Jensen and Rohwer, 1966), the drug-Stroop task measures the attentional interference induced by color-naming of drug vs. non-drug related words. This drug-related attentional interference manifests as prolonged response times

(Ersche et al., 2010) and/or altered neural activation in the brain's reward/salience circuitry [OFC, anterior cingulate, striatum, and midbrain (Goldstein et al., 2009a, 2009b; Smith and Ersche, 2014)]. However, while the Go/No-Go task captures response selection ability (Raud et al., 2020), it does not measure the ability to stop after response initiation, and the drug-Stroop task does not create an inherent inhibitory control demand, rendering both task types insufficient in informing potential lapses in self-control under a motivationally challenging state, such as craving.

The stop-signal task (SST) permits the investigation of inhibitory control by estimating the competition between the "Go" and "Stop" processes (Verbruggen and Logan, 2008), and has previously demonstrated the neural correlates of inhibitory control in drug addiction (Li et al., 2008, 2009; Matuskey et al., 2013; Elton et al., 2014; Sjoerds et al., 2014; Hu et al., 2015; Harlé et al., 2016, 2019; Wang et al., 2018; Zhang et al., 2018; Sakoglu et al., 2019; Zhukovsky et al., 2021). However, a gap remains in the modulation of inhibitory control by drug cue salience for the inspection of their interaction at the brain level. In individuals with CUD and matched HC, we present results of a novel stop-signal task (SST) that allowed for the parametric/trial-by-trial modulation of inhibitory control by salient drug, other salient non-drug (e.g., food), and neutral cues (words) during fMRI. Further, we conservatively pre-selected our data to abide by recent recommendations of best practices in estimating stopping ability (Verbruggen et al., 2019). We probed three core hypotheses: 1) Regardless of cue type and group, prefrontal regions would drive inhibitory control processes on this hybrid task; 2) inhibitory control-related prefrontal signaling would be altered in the CUD group; and 3) the dlPFC (and other inhibitory PFC regions, e.g., the IFG) would be crucial for inhibitory control under drug cue reactivity in CUD, and this effect would be supported by a link with cocaine use severity.

Materials and Methods

Participants

Participants were recruited using flyers, newspaper ads, and by word of mouth. From a dataset of 79 participants with valid behavioral data, we pre-selected 52 demographically-matched individuals (n=26 per group, 43 males, mean age: 43.4 ± 7.6; see Behavioral data analysis and BOLD-fMRI data analysis sections for details, and Table 1 for sample profile). Participants underwent a series of clinical and neuropsychological assessments delivered by trained staff under a clinical psychologist's supervision. These interviews included the Structured Clinical Interview for DSM IV for Axis I Disorders (American Psychiatric Association, 2013); the Addiction Severity Index (McLellan et al., 1992)—a semi-structured interview instrument that assesses the severity as well as recent and lifetime history of alcohol- and drug-related problems; the Cocaine Selective Severity Assessment (Kampman et al., 1998) for evaluating cocaine abstinence/withdrawal signs and symptoms (i.e., sleep impairment, anxiety, energy levels, craving and depressive symptoms) 24 h within time of interview; the 5-item Cocaine Craving Questionnaire (Tiffany et al., 1993); and the 5-item Severity of Dependence Scale (Gossop et al., 1992). A brief physical examination encompassing height, weight, urine drug toxicology, breath alcohol and carbon monoxide (for recent cigarette use) levels, and medical history, were also obtained by trained research staff.

Participants were excluded for the following: 1) history of major psychiatric disorders [barring other substance use disorders and highly comorbid illnesses such as post-traumatic stress disorder (PTSD) for CUD, and nicotine dependence for HC]; 2) history of seizures or other central nervous system disorders; 3) cardiovascular, endocrinological, metabolic, oncological, or autoimmune disease; 4) MRI contraindications; 5) presence of psychoactive drugs or their metabolites (except for cocaine in the CUD group) in urine assays; 6) evidence of alcohol and/or any other drug-related intoxication at the time of participation; 7) positive pregnancy test (determined via a urine assay); and 8) color blindness [assessed with the Ishihara color blindness test (Clark, 1924)].

All participants in the CUD group met criteria for substance use disorder (with cocaine and/or crack cocaine as the primary substance of choice, 23 meeting criteria for dependence, and three for abuse). Urine screen results confirmed the presence of cocaine in 22 participants in the CUD group. Urine screens for all other drugs were negative (the HC participants tested negative for all drugs, including cocaine). Comorbid diagnoses within CUD included current intermittent explosive disorder (N = 5), PTSD in full remission (N = 1), specific phobias (N = 2), marijuana dependence (N = 13), alcohol abuse and/or dependence (N = 26), opioid dependence (N = 8), amphetamine dependence (N = 1), hallucinogen abuse and/or dependence (N = 2), and polysubstance dependence (N = 3). Diagnoses among HC included intermittent explosive disorder (current: N = 10, past: N = 1), PTSD in full remission (N = 2), specific phobias (N = 1), alcohol dependence (N = 6), and marijuana abuse and/or dependence (N = 3). All substance use comorbidities were in full remission (except for one CUD participant who met criteria for marijuana dependence, partial remission). The Icahn School of Medicine at Mount Sinai institutional review board approved all study procedures. Participants received full information about the research and provided written consent in accordance with the institutional review board of the Icahn School of Medicine at Mount Sinai.

[Table 1]

Experimental Design and Statistical Analysis

Emotional Stop-Signal Task

In the traditional SST, participants are instructed to respond to a frequent neutral Go signal as quickly as possible, and inhibit responses to this cue when it is followed by a rare stop-signal [e.g., a visual cue superimposed on the Go signal, or an auditory tone (Verbruggen and Logan, 2008); see Figure 1, left].

[Figure 1]

Here, during fMRI, we presented drug, food, and threat-related words in addition to neutral words as the Go signals in a modified emotional SST task (eSST; see Figure 1, right). These words were matched in length and frequency in the English language [mean frequency: drug words = 23.69, food words = 15.70, threat words = 19.87, neutral words = 21.97; (Francis et al., 1982)]. Each trial started with a fixation cross that jittered in duration between 2000 and 2600 ms to minimize stimulus anticipation and improve signal to noise ratio (Wager and Nichols, 2003), which was then followed by a drug, food, threat, or neutral word in white text over a black background (1000 ms). Next, the word in white text changed in color to blue or green, to which the participants were instructed to respond with their right (for blue font) or left (for green font) index finger using MR compatible response gloves. These Go trials comprised 50% of trials; in 25% of trials, a stop-signal followed the change in color, such that the blue or green font turned red after a variable delay (i.e., the stop-signal delay, or SSD). This change instructed the participants to suppress their response (when the word color turned red; see Figure 1, right bottom). The SSD was set to an initial duration of 250 ms and adjusted in parallel to the participant's stopping ability for each cue type (yielding four independent SSD adjustments to precisely estimate stopping speed to each cue). When the participant successfully stopped, the SSD increased by 50 ms (making the next stop trial more difficult), and when the participant failed to stop, the SSD decreased by 50 ms (making the next stop trial easier). The remaining 25% of trials were empty trials in the form of a fixation cross (2 s; same as the Go trial duration). Participants underwent four runs of this task, with each run containing 48 Go and 24 Stop trials (18 trials in each word category per run). After the MRI session, participants were instructed to rate each word using a 5-point scale on valence ["Please rate how you currently feel about the above words from PLEASANT (leftmost) to UNPLEASANT (rightmost) using the scale."] and arousal ["Please rate how emotional you currently feel about the above words from VERY EMOTIONAL (leftmost) to CALM (rightmost) using the scale."].

MRI data acquisition

Scanning was conducted on a Siemens 3T MAGNETOM Skyra (Siemens, Erlangen, Germany), using a 32-channel head coil. The BOLD-fMRI responses were measured as a function of time using a T2*-weighted single shot multi-band accelerated gradient-echo EPI sequence [TE/TR=35/1000 ms, 2.1 mm isotropic resolution, no gap, 70 axial slices for whole brain (14.7 cm) coverage, FOV 206 × 181 mm, matrix size 96 × 84, 60°-flip angle (approximately Ernst angle), multi-band factor of 7, blipped CAIPIRINHA phase-encoding shift=FOV/3, ~2 kHz/Pixel bandwidth with ramp sampling, echo spacing 0.68 ms, and echo train length 57.1 ms]. Each of the four fMRI task runs were approximately 6 m 30 s in length, totaling about 26 m. T1- weighted anatomical images were acquired using a 3D MPRAGE sequence [FOV 256 × 256 × 179 mm^3, 0.8 mm isotropic resolution, TR/TE/TI=2400/2.07/1000 ms, flip angle 8° with binomial (1, −1) fat saturation, bandwidth 240 Hz/pixel, echo spacing 7.6 ms, and in-plane acceleration (GRAPPA) factor of 2, with a total acquisition time of ~7]. The 90-m scan session included additional procedures (presented in a randomized order to circumvent possible order effects) reported elsewhere (Moeller et al., 2018).

MRI data preprocessing

Raw fMRI data in DICOM format were converted to NIFTI using dcm2niix (Li et al., 2016) and adapted to Brain Imaging Data Structure (BIDS) standards to enhance neuroimaging data portability and reproducibility (Gorgolewski et al., 2016). BIDS-validated data were then preprocessed via the Nipype-based fMRIPrep pipeline (version 1.5.0) (Gorgolewski et al., 2011; Esteban et al., 2019). FMRIPrep is a robust fMRI preprocessing pipeline that recruits tools from well-established neuroimaging software (e.g., FSL, Freesurfer, AFNI) to standardize and optimize fMRI preprocessing (Esteban et al., 2019). FMRIPrep's workflow is summarized as follows: structural images were corrected for intensity non-uniformity and skull-stripped using ANTS (Tustison et al., 2010). These structural images were spatially normalized to the ICBM 152 Nonlinear Asymmetrical template via nonlinear registration using ANTS (Avants et al., 2008; Fonov et al., 2009). Brain tissue was segmented into white matter, gray matter, and

cerebrospinal fluid using FSL's FAST (Zhang et al., 2001). Functional data were corrected for motion artifacts using FSL's MCFLIRT and for distortion using spin-echo field maps acquired in opposing phase encoding directions via AFNI's 3dQwarp (Cox, 1996; Jenkinson et al., 2002). Motion and distortion corrected images were then co-registered to the participant's structural images using boundary-based registration with 9 degrees of freedom via Freesurfer (Greve and Fischl, 2009). These correction, transformation, and registration steps were integrated into a single step transformation workflow using ANTS. In addition to the fMRIPrep workflow, we identified volumes with spikes in translation and rotation parameters in relation to a reference volume. Using a typical boxplot threshold (75th percentile + 1.5 * interquartile range) via FSL's *fsl_motion_outliers* package, we regressed out an average of 5.92% of outlier volumes in each run (range: 0.51%-14.32%). Average number of outlier volumes regressed out from participants in the CUD group did not significantly differ from those in the HC group, $t(50) = 0.71$, $p = .483$. As a result, there remained no substantial volume-to-volume movement (framewise displacement was below voxel dimensions at mean motion: 0.05 mm; maximum motion: 0.17 mm), with no significant differences across groups, $t(50) = 0.61$, $p = .542$. The preprocessed data from the fMRIPrep pipeline were filtered with a high-pass filter (100 s cutoff) to ignore scanner drift, and spatially smoothed using a Gaussian kernel (5 mm full-width at half maximum) to improve signal to noise ratio. We set an a priori threshold for mean voxel intensity values in all preprocessed images for quality control: BOLD runs with mean voxel intensity at 3 standard deviations above or below the mean of the sample were removed from analyses to mitigate the potential effects of scanner artifacts (excluded CUD n = 2).

Behavioral data analysis

A core assumption of the stop-signal paradigm is that Go and Stop processes are in competition to exert control over motor output—a phenomenon described by the horse-race model of response inhibition (Logan and Cowan, 1984). To ensure that we accurately estimated stopping ability using our novel stop-

signal task, we followed a recently documented consensus guide for upholding the validity of the horse-race model while analyzing stop-signal task data (Verbruggen et al., 2019). We used the integration method to calculate SSRT, in that we identified the nth RT in the Go RT distribution, with n being the number of Go RTs multiplied by the proportion of trials where a response was made to a stop-signal, which represents the finishing time of the stopping process (and improves on the common "mean RT" method) (Verbruggen et al., 2019). Accordingly, we only included data from task runs in which the participant displayed mean Go accuracy of 60% or higher, mean Stop accuracy greater than or equal to 25% but less than or equal to 75% (ensuring that the SSD indeed resulted in a competition between Go and Stop processes), and positive mean SSRT. After removing task runs in which the above criteria were violated, there were no significant differences between groups in number of valid task runs [$t(77) = 0.45$, $p = .652$]. We then matched CUD and HC participants on age, years of education, and verbal IQ using the R package *MatchIt* (Ho et al., 2011) to maintain a comparable pair of samples (excluded participants: HC n = 13). Due to the verbal nature of this task and concerns about lateralization differences in left-handed participants, we only included right-handed participants in the fMRI analyses (i.e., Edinburgh Handedness Inventory score > 75%; excluded participants: CUD n = 5, HC n = 4).

We performed a mixed-design repeated measures ANOVA, with SSRT as the dependent variable, Group (CUD, HC) as the between- and Cue (Drug, Food, Threat, Neutral) as the within-subject factors. We followed up on significant interactions with post-hoc t-tests where appropriate. Because the data were pre-selected based on Go and Stop accuracy performance, we did not focus on statistical differences based on these variables. We further explored the behavioral and the clinical profile of our participants by using selected demographics and drug use severity measures in correlational analyses with average and Drug SSRT using Spearmen's correlations, Holm-corrected for multiple comparisons. Post-task ratings to the word cues were entered into two-way ANOVAs (Group as between-, Cue as within-subject

factors, valence and arousal as separate dependent variables) to test whether participants differentially perceived the valence and arousal of the words across cue types and groups.

BOLD-*fMRI data analysis*

Parameter estimates were generated for each participant using the general linear model (GLM) approach via FSL's FEAT (version 5.98; Woolrich et al., 2001). Four events (Go_Success for successful Go responses, Go_Fail for missed Go trials or response selection errors, Stop_Success for successfully inhibited responses following a stop-signal, and Stop_Fail for failed inhibitions following a stop-signal) per cue type (drug, food, threat, and neutral) were modeled, yielding 16 cue-specific regressors (e.g., Drug_Stop_Success, Food_Stop_Fail, etc.). Regressors were sampled from the onset of the corresponding trials' Go signals using 1 s events and convolved with a canonical hemodynamic response function along with their temporal derivatives to be entered into the GLM. Fixation events were not modeled, in that they contributed to the task baseline for linear contrasts—a practice that is in line with prior analyses of the SST (Aron and Poldrack, 2006). We used each cue's Go_Fail events and the *fsl_motion_outlier* outputs denoting volumes with excessive spikes in intensity as regressors of no interest. We further removed individuals who did not yield complete fMRI regressors to represent behavioral performance in line with the horse-race model assumptions. For example, if a participant's non-missing task runs were insufficient in yielding all the necessary task events (e.g., a missing Drug_Stop_Success because the participant had no successful stops during Drug cues in their only remaining run), we excluded the participant from analyses (excluded participants: HC n = 3). We based our behavioral and neural analyses on a final pool of 52 participants for consistency and examinations of behavioral performance vis-à-vis BOLD activity (see Table 1 for sample profile).

In each of the four runs, the first level analyses comprised all regressors' contrasts with baseline (e.g., Drug_Go_Success > Baseline to examine Go-related processes in drug cue trials). Importantly, we used

Stop_Success > Stop_Fail as the hallmark contrast of inhibitory control. Thus, the first-level GLM included contrasts for detecting cue-general (Stop_Success > Stop_Fail regardless of cue type) and cue-specific (e.g., Drug_Stop_Success > Drug_Stop_Fail) inhibitory control processes. We contrasted drug with food—a competing, non-drug positively valenced reinforcer [i.e., (Drug_Stop_Success > Drug_Stop_Fail) > (Food_Stop_Success > Food_Stop_Fail)] to focus specifically on regulation of salient drug versus non-drug-related inhibitory control—a practice with precedence and specificity to predicting drug use and correlating with other non-lab drug use measures in CUD (Martinez et al., 2009; Moeller et al., 2009, 2010, 2018). We also contrasted drug-related inhibition with the non-salient neutral category of cues [i.e., (Drug_Stop_Success > Drug_Stop_Fail) > (Neutral_Stop_Success > Neutral_Stop_Fail)], permitting the examination of drug-related arousal. These contrasts in each run were entered into a fixed-effects model to generate aggregate parameter estimates representing general and cue-specific inhibitory control processes at the participant level. Other iterations of cue contrasts (e.g., Food > Threat, Drug > Threat) were also modeled for consistency, although we did not have an a priori interest in these comparisons for the current purposes. In other words, although we used in the GLM threat cues as the non-drug category that accounts for the potentially negative valence of drug cues, direct comparisons involving threat are outside the scope of our primary interests regarding the iRISA interaction for the current purposes.

To investigate the neural mechanisms of inhibitory control across the CUD and HC groups, the resulting participant-level activation maps were analyzed in a higher level analysis using FSL's FLAME 1 & 2 (FMRIB's Local Analysis of Mixed Effects), which improves group-level variance estimates via Markov Chain Monte Carlo simulations to allow for population inferences (Beckmann et al., 2003). We chose a cluster defining threshold of $p < .001$, corrected to a cluster-extent threshold of $p < .05$, in line with common practices to minimize Type I error (Eklund et al., 2016).

To detect cue-general inhibitory control related neural activation, directly associated with stopping ability, we performed a similar higher-level analysis with identical thresholding and variance estimation methods, with the addition of mean SSRT as a covariate. We also included cue-specific SSRT covariates that mirrored the BOLD contrasts for cue comparisons. For instance, a covariate containing "Drug SSRT minus Food SSRT" values was created to detect activation patterns during drug versus food inhibition that varied based on behavioral performance to drug versus food cues. Finally, we used select drug use severity measures (i.e., years of cocaine use, frequency of use in past 30 days, days since last use, severity of dependence, withdrawal, and craving) to reveal whether these severity estimates correlated with any regional activation in the brain during drug cue-related inhibitory control.

Results

Behavioral results

The mixed-design repeated measures ANOVA of SSRT revealed no main effect of Group, $F(1,50) = 3.13$, $p = .083$, no main effect of Cue, $F(3,150) = 0.65$, $p = .584$, but a significant Group x Cue interaction, $F(3,150) = 3.15$, $p = .027$, where HC were exhibited prolonged SSRT to Food and Neutral cues (see Figure 2 and Table 2). Descriptive statistics for Go and Stop accuracy and Go RT-related group differences are included in Table 2.

[Figure 2]

[Table 2]

The total score on Severity of Dependence Scale positively correlated with overall SSRT (Spearman's $r = .40$, $p = .043$, Holm-corrected), such that higher severity of cocaine dependence was associated with slower SSRT (worse performance). No other clinical measure showed a significant correlation with behavior (all ps > .05).

Due to missing data, we were able to extract post-task word rating data from 45 out of the 52 participants included in the analyses (CUD: n = 21; HC: n = 24). A two-way ANOVA with valence as the dependent variable, Group as between-, and Cue as within-subject factors revealed no main effect of Group, $F(1,37) = 0.92$, $p = .343$, a significant main effect of Cue, $F(3,37) = 19.75$, $p < .001$, and no Group x Cue interaction, $F(3,37) = 0.25$, $p = .859$. Pairwise comparisons of valence ratings between cue types across all participants indicated the following (from most to least positive): Food > Neutral > Drug > Threat, $t(44) \geq 7.27$, $p < .001$. An identical two-way ANOVA with arousal as the dependent variable revealed no main effect of Group, $F(1,37) = 1.64$, $p = .209$, a significant main effect of Cue, $F(3,37) = 5.53$, $p = .003$, and no Group x Cue interaction, $F(3,37) = 2.28$, $p = .095$. Pairwise comparisons of arousal ratings between cue types across all participants indicated the following (from most to least arousing): Threat > Drug > Neutral, $t(44) \geq 2.58$, $p \leq .013$; Food cues, although greater than neutral cues, $t(44) = 2.33$, p = .024, did not significantly differ in arousal ratings from Threat or Drug cues (both *p*s > .05). Thus, across all subjects, drug words were rated as more negative than food words; their level of arousal did not differ.

BOLD-fMRI results

Inhibitory control-related neural signaling (across all participants)

The whole-brain analysis of overall inhibitory control across all participants (i.e., neural signaling during Stop_Success > Stop_Fail regardless of cue type and group) yielded significant clusters in classical inhibitory control-associated regions, such as right vmPFC (Brodmann's Area, or BA10), left OFC (BA47), left IFG (BA45), right frontal pole/dmPFC (BA8; among several other regions listed in Table 3, top). Next, we used mean SSRT (regardless of cue type) as a covariate to detect cue-general inhibitory control and found significant clusters namely in the right frontal pole/anterior PFC (BA10), right paracingulate gyrus

(BA9), bilateral middle frontal gyrus/dlPFC (BA8 in both hemispheres), and among several others (see Table 3, bottom).

[Table 3]

Group differences in inhibitory control-related neural signaling

Whole-brain analysis of overall inhibitory control (regardless of cue type) between groups revealed decreased activation in the CUD group relative to HC in the left frontal pole/dmPFC (BA10: MNI space -4, 57, 21; peak Z = 5.04, 97 voxels) and left lateral occipital cortex (BA39: MNI space -42, -63, 27; peak Z = 4.16, 70 voxels; see Figure 3).

[Figure 3]

We also used mean SSRT as a covariate to determine potential group differences in the brain regions that correlated with stopping ability, and found significantly higher activations in CUD compared to HC in the posterior cingulate (BA31: MNI space -2, -35, 40; peak Z = 4.28, 54 voxels), left precuneus (BA7: MNI space -8, -66, 52; peak Z = 4.88, 105 voxels), and cuneal cortices (BA19: MNI space -23, -72, 19; peak Z = 4.22, 59 voxels), such that the higher the activity in these regions, the slower the SSRT (worse performance) specifically in CUD.

In sum, these results suggest that in CUD compared to HC the dmPFC is hypoactivated during inhibitory control, and greater activity in the posterior cingular/parietal regions is more closely associated with worse stopping ability.

Group differences in inhibitory control-related neural signaling under drug cue reactivity

Importantly, to capture the hypothesized iRISA interaction, we performed whole-brain analyses that focused on group differences in BOLD signal during drug versus food related inhibitory control, which

allowed us to examine specific neural responses to drug cue reactivity compared to another salient pleasant (positively valenced) cue that is associated with consummatory behavior. The results revealed significant left dlPFC hypoactivations in the CUD group compared to HC during Drug > Food-related inhibition (BA8: MNI space -53, 12, 38; peak Z = 3.89, 62 voxels; see Figure 4), suggesting that specifically in CUD, this region exhibited decreased signaling during the inhibitory control of drug words (which were rated as more arousing and negatively valenced compared to food words in both groups). Similar analyses with Drug > Neutral-related inhibition did not yield significant results.

[Figure 4]

We also used Drug SSRT > Food SSRT as a covariate to determine group differences in which brain cue-sensitive inhibitory control regions correlated with Drug > Food-related stopping ability. A whole brain correlation found that the right superior lateral occipital cortex activity (BA39: MNI space 46, -66, 21; peak Z = 4.09, 61 voxels) negatively correlated with Drug > Food SSRT in HC compared to CUD, such that increased activity was associated with quicker stopping to drug compared to food cues in HC, and this correlation was significantly stronger than in the CUD group. Similar analyses with Drug > Neutral SSRT did not yield significant group differences in correlations.

Cocaine use severity and inhibitory control-related signaling under drug cue reactivity in the CUD group

CUD-focused analyses of drug use severity (the six cocaine use variables in Table 1) were conducted via unbiased, whole-brain correlations, effectively localizing the regions in which these drug use measures tracked the BOLD signal during drug-related (Drug > Food and Drug > Neutral) inhibition (see Table 4). Most notably, we found a significant positive correlation between recent frequency of use (days in the past month) and Drug > Food inhibition-related right OFC (BA47), right superior frontal gyrus/dmPFC (BA6) and left dlPFC (BA6) activity in the CUD group (see Figure 5). Using this same contrast (i.e., Drug > Food), a positive correlation was also observed with cocaine craving ratings in the right dlPFC (BA9),

right IFG (BA44), and right middle temporal gyrus (BA21). Consistent with this direction of associations, negative correlations were observed with length of abstinence in the right anterior PFC (BA10), right dlPFC (BA44), and right precentral gyrus (BA6). Together, these results suggest that the more frequent the recent cocaine use, the higher the craving, and the shorter the abstinence, the higher the activity mainly in PFC regions during drug compared to food-related inhibitory control. Similarly, Drug > Neutral inhibition related BOLD signal positively correlated with recent cocaine use frequency in the left dlPFC (BA8) and cocaine craving in the left anterior PFC (BA8), left dlPFC (BA10), right dmPFC (BA6), left IFG (BA44), and the right hippocampus. Thus, similarly to the Drug > Food contrast, the Drug > Neutral contrast showed that higher prefrontal cortical activations (during drug compared to neutral-related inhibitory control) are related to more frequent cocaine use and higher craving.

[Figure 5]

Discussion

Despite consistent evidence for inhibitory control and salience attribution impairments in individuals with substance use disorders [see reviews: (Zilverstand et al., 2018; Ceceli et al., 2021)], our understanding of how these hallmark addiction symptoms interact, and the neural underpinnings of this interaction, remains incomplete. Here, a novel fMRI SST permitted the neurobehavioral examination of the interaction between inhibitory control and salient drug and non-drug cue processing in CUD. First, significant activations in the vmPFC, OFC, IFG, and dmPFC during successful compared to failed stops, independent of cue type or group, support our first aim to validate this novel task, showing its consistency with the PFC's role in driving inhibitory control (Verbruggen and Logan, 2008). Hypoactivations in the dmPFC during overall inhibitory control in the highly pre-selected group of individuals with CUD support our second hypothesis, contributing to the reliably documented decreased PFC signaling during a wide-range of neuropsychological functions, including response inhibition in this

population (Zilverstand et al., 2018). Third, and most importantly, we revealed evidence for the iRISA interaction in the CUD brain. Despite group similarities in both drug cue behavioral performance and arousal/valence ratings, and despite meeting the stringent criteria for SST's horse-race model assumptions, compared to the HC group, CUD participants showed decreased dlPFC function during drug vs. food (a consummatory non-drug positive reinforcer) cue inhibition. The lower these dlPFC responses to drug vs. food cues, the lower the drug use severity encompassing less frequency of recent use, lower craving and longer abstinence.

The OFC and IFG activations during successful stopping in all participants regardless of cue type suggest that our novel task effectively captures inhibitory control in the brain. These regions are known to comprise the brain's cognitive control network, with specific involvement in the suppression of inappropriate behaviors, especially during the SST (Aron and Poldrack, 2006; Aron et al., 2007; Brockett and Roesch, 2021). The significant dmPFC hypoactivations in CUD during overall inhibitory control agree with previous evidence where a similar dmPFC region was also hypoactivated in CUD compared to HC during inhibitory control—interestingly during Go/No-Go performance with neutral letter stimuli (Hester and Garavan, 2004). Notably, the lack of behavioral performance deficits in CUD and comparable valence and arousal ratings between groups suggest that these PFC hypoactivations during inhibitory control are not driven by compromises in task comprehension, performance, or perception of stimuli.

Agnostic to group and cue type, mean SSRT was positively correlated with dlPFC and paracingulate activity (among other regions), suggesting increased activation in these regions with slower stopping. This result disagrees with the direction of the correlation reported in several studies (Aron and Poldrack, 2006; Li et al., 2006a; Zhao et al., 2019; Chevrier and Schachar, 2020; Lee and Hsieh, 2017; but see de Wit et al., 2012). These studies largely reported a negative correlation between SSRT and cortical and subcortical activity (namely in the PFC and basal ganglia) including the default mode network—a set of brain regions that exhibit low-frequency oscillations at "rest", typically associated with self-referential

thought (Raichle et al., 2001). The source of the different direction of correlations is not clear but could be attributed to the variability introduced by the word stimuli, which may more readily elicit self-referential brain activity, especially in CUD. Indeed, compared to HC, in CUD the precuneus and posterior cingulate—two of the functional hubs of the default mode network (Raichle et al., 2001; Utevsky et al., 2014)—were more positively correlated with SSRT, suggesting that those who were slower to stop also exhibited higher default mode network activity during inhibitory control.

Most importantly, for the first time we demonstrate the neural signature of the iRISA interaction in CUD. In behaviorally comparable CUD and HC samples, we found evidence for decreased inhibitory control signal in the dlPFC only in CUD during drug cues relative to a non-drug reinforcer (food cues). One explanation for this dlPFC deactivation invokes the suppression of salient drug cue reactivity, in line with the dlPFC's role in orchestrating craving, potentially by modulating the OFC, which combines the value of the craving-inducing cues with affective states and drug availability (George and Koob, 2013), overall leading to decreased craving when the dlPFC is inactivated. Indeed, smokers who underwent dlPFC inactivation via transcranial magnetic stimulation (1 Hz) displayed reduced craving when cigarettes were immediately available, and dlPFC inactivation decreased craving-related OFC activity during a smoking cue-reactivity task (Hayashi et al., 2013). Adopting this perspective, our results suggest that to resemble the HC behavioral performance, the CUD group needed to decrease dlPFC signaling during inhibitory control especially during the potentially craving enhancing drug (vs. other salient) cues. Accordingly, those CUD individuals with the most severe drug use patterns (i.e., more frequent recent use, higher craving, and shorter abstinence) were less likely to exhibit decreased dlPFC (and OFC) response in the face of drug (vs. food) cues. It remains to be tested whether this pattern is a biomarker of resilience, whereby the ability to exert control during drug cue reactivity in the lab predicts craving and drug use outside the lab. An alternative explanation invokes self-medication (and vulnerability)—whereby those with more frequent recent cocaine use may be normalizing underlying neurocognitive dysfunction by

increasing dlPFC activity, masking (with cocaine, a stimulant) the neuropsychological deficits associated with cocaine addiction (Woicik et al., 2009; Parvaz et al., 2012, 2015). This latter interpretation is more consistent with the expected direction of effect for the dlPFC, whereby reduced activation during inhibitory control is a marker of a deficit. Accordingly, lateral occipital activity was associated with quicker SSRT in HC (but not CUD) in the drug context, which, combined with the relationship between slower SSRT and higher default mode network activity in CUD, suggests that these posterior regions may be compensating by aiding performance in HC but not CUD. Inhibitory control-related comparisons between recent cocaine users and abstainers (or as a function of abstinence longitudinally) would be needed to contrast these perspectives in future efforts.

Limitations of the present study include high rates of data exclusion due to the stringent SSRT estimation parameters. While data filtering to validate SSRT is integral in capturing inhibitory control in the lab, performance feedback between task runs to remind participants of the instructions (e.g., ensuring that the participant does not wait for the stop-signal) may minimize the loss of data and statistical power (Verbruggen et al., 2019). Furthermore, although behavioral investigations show inhibitory slowing to emotionally salient stimuli in the general population (Verbruggen and Houwer, 2007; Herbert and Sütterlin, 2011; Kalanthroff et al., 2013; Ding et al., 2020), we found prolonged SSRT in response to food and neutral cues in HC, with no evidence for slowing for the other arousing cue types or in CUD. Generally, while CUD may be expected to perform worse than HC in this task, evidence for (Fillmore and Rush, 2002; Li et al., 2006b; Wang et al., 2018) and against (Li et al., 2008; Vonmoos et al., 2013; Chao et al., 2019) prolonged SSRT in CUD vs. HC exists, warranting further inquiry into behavioral inhibitory performance in this population. Using visual cues (e.g., drug use images or video clips) may have more effectively induced sustained cue-reactivity than word stimuli; however, the word stimuli were preferred for our trial-by-trial design and for rendering verbal features such as length and frequency uniform between conditions, which may be further improved by equating arousal within each

valence category. These results should also be replicated with more sex-balanced samples that can inform about potential sex differences in the neural mechanisms of inhibitory control. Lastly, although we statistically accounted for neural responses to threat cues, in-depth analyses of these activations await samples that better represent relevant comorbidities (e.g., intermittent explosive disorder).

To the best of our knowledge, this is the first report of the brain systems that regulate inhibitory control under drug cue reactivity in human cocaine addiction. Using a novel SST to better represent the addiction experience in humans, where reminders of cocaine use can exert control over behavior, we were able to reveal the neural mechanisms of the iRISA interaction. Our results ascribe an important role to the dlPFC in the control of behavior under drug cue salience. Specifically, although the task promotes increased PFC function in cognitive control-related regions, drug vs. food cue-related hypoactivations were evident in CUD compared to HC, as associated with less frequent recent use, craving and with longer abstinence. This dlPFC drug cue suppression may be a marker of resilience (dampening craving-related processes) or a signature of vulnerability (where cocaine is used to normalize impaired cognitive processes in the short term, yet with long-term negative consequences). Together, our results point to the mechanisms behind lapses in self-control when faced with a salient drug context in addicted individuals. A closer examination with only treatment-seeking individuals is warranted to test whether these neurobiological patterns are related to deviations from treatment goals. Results could also offer the possibility to refine neuromodulation to mitigate the effects on self-control of craving and other drug-related behaviors in drug addiction.

References

American Psychiatric Association (2013) Diagnostic and Statistical Manual of Mental Disorders, Fifth Edition. American Psychiatric Association. Available at: http://psychiatryonline.org/doi/book/10.1176/appi.books.9780890425596 [Accessed December 8, 2015].

Ames SL, Wong SW, Bechara A, Cappelli C, Dust M, Grenard J L, Stacy AW (2014) Neural Correlates of a Go/NoGo Task with Alcohol Stimuli in Light and Heavy Young Drinkers. Behav Brain Res 0:382–389.

Aron AR, Behrens TE, Smith S, Frank MJ, Poldrack RA (2007) Triangulating a Cognitive Control Network Using Diffusion-Weighted Magnetic Resonance Imaging (MRI) and Functional MRI. J Neurosci 27:3743–3752.

Aron AR, Poldrack RA (2006) Cortical and Subcortical Contributions to Stop Signal Response Inhibition: Role of the Subthalamic Nucleus. J Neurosci 26:2424–2433.

Avants BB, Epstein CL, Grossman M, Gee JC (2008) Symmetric diffeomorphic image registration with cross-correlation: Evaluating automated labeling of elderly and neurodegenerative brain. Medical Image Analysis 12:26–41.

Beckmann CF, Jenkinson M, Smith SM (2003) General multilevel linear modeling for group analysis in FMRI. Neuroimage 20:1052–1063.

Brockett AT, Roesch MR (2021) The ever-changing OFC landscape: What neural signals in OFC can tell us about inhibitory control. Behav Neurosci 135:129–137.

Carpenter KM, Schreiber E, Church S, McDowell D (2006) Drug Stroop performance: Relationships with primary substance of use and treatment outcome in a drug-dependent outpatient sample. Addictive Behaviors 31:174–181.

Ceceli AO, Bradberry CW, Goldstein RZ (2021) The neurobiology of drug addiction: cross-species insights into the dysfunction and recovery of the prefrontal cortex. Neuropsychopharmacology.

Chao T, Haney M, Cooper ZD, Vadhan NP, Van Dam NT, Van Snellenberg J, Bedi G (2019) Cognitive function in aging cocaine smokers. J Psychopharmacol 33:801–810.

Chevrier A, Schachar RJ (2020) BOLD differences normally attributed to inhibitory control predict symptoms, not task-directed inhibitory control in ADHD. J Neurodevelop Disord 12:8.

Clark JH (1924) The Ishihara Test for Color Blindness. American Journal of Physiological Optics 5:269–276.

Cox RW (1996) AFNI: Software for Analysis and Visualization of Functional Magnetic Resonance Neuroimages. Computers and Biomedical Research 29:162–173.

Czapla M, Baeuchl C, Simon JJ, Richter B, Kluge M, Friederich H-C, Mann K, Herpertz SC, Loeber S (2017) Do alcohol-dependent patients show different neural activation during response inhibition than healthy controls in an alcohol-related fMRI go/no-go-task? Psychopharmacology 234:1001–1015.

de Wit SJ, de Vries FE, van der Werf YD, Cath DC, Heslenfeld DJ, Veltman EM, van Balkom AJLM, Veltman DJ, van den Heuvel OA (2012) Presupplementary Motor Area Hyperactivity During Response Inhibition: A Candidate Endophenotype of Obsessive-Compulsive Disorder. AJP 169:1100–1108.

DeVito EE, Kiluk BD, Nich C, Mouratidis M, Carroll KM (2018) Drug Stroop: Mechanisms of response to computerized cognitive behavioral therapy for cocaine dependence in a randomized clinical trial. Drug Alcohol Depend 183:162–168.

Ding J, Wang Y, Wang C, d'Oleire Uquillas F, He Q, Cheng L, Zou Z (2020) Negative Impact of Sadness on Response Inhibition in Females: An Explicit Emotional Stop Signal Task fMRI Study. Front Behav Neurosci 14 Available at: https://www.frontiersin.org/articles/10.3389/fnbeh.2020.00119/full?report=reader [Accessed February 6, 2021].

Eklund A, Nichols TE, Knutsson H (2016) Cluster failure: Why fMRI inferences for spatial extent have inflated false-positive rates. Proc Natl Acad Sci USA 113:7900–7905.

Elton A, Young J, Smitherman S, Gross RE, Mletzko T, Kilts CD (2014) Neural network activation during a stop-signal task discriminates cocaine-dependent from non-drug-abusing men. Addiction Biology 19:427–438.

Ersche KD, Bullmore ET, Craig KJ, Shabbir SS, Abbott S, Müller U, Ooi C, Suckling J, Barnes A, Sahakian BJ, Merlo-Pich EV, Robbins TW (2010) Influence of Compulsivity of Drug Abuse on Dopaminergic Modulation of Attentional Bias in Stimulant Dependence. Arch Gen Psychiatry 67:632–644.

Esteban O, Markiewicz CJ, Blair RW, Moodie CA, Isik AI, Erramuzpe A, Kent JD, Goncalves M, DuPre E, Snyder M, Oya H, Ghosh SS, Wright J, Durnez J, Poldrack RA, Gorgolewski KJ (2019) fMRIPrep: a robust preprocessing pipeline for functional MRI. Nat Methods 16:111–116.

Fillmore MT, Rush CR (2002) Impaired inhibitory control of behavior in chronic cocaine users. Drug and Alcohol Dependence 66:265–273.

Fonov V, Evans A, McKinstry R, Almli C, Collins D (2009) Unbiased nonlinear average age-appropriate brain templates from birth to adulthood. NeuroImage 47:S102.

Francis W, Kučera H, Mackie AW (1982) Frequency Analysis of English Usage: Lexicon and Grammar. Boston: Houghton Mifflin.

George O, Koob GF (2013) Control of craving by the prefrontal cortex. Proc Natl Acad Sci U S A 110:4165–4166.

Gilman JM, Radoman M, Schuster RM, Pachas G, Azzouz N, Fava M, Evins AE (2018) Anterior insula activation during inhibition to smoking cues is associated with ability to maintain tobacco abstinence. Addict Behav Rep 7:40–46.

Goldstein RZ, Alia-Klein N, Tomasi D, Carrillo JH, Maloney T, Woicik PA, Wang R, Telang F, Volkow ND (2009a) Anterior cingulate cortex hypoactivations to an emotionally salient task in cocaine addiction. Proc Natl Acad Sci U S A 106:9453–9458.

Goldstein RZ, Tomasi D, Alia-Klein N, Carrillo JH, Maloney T, Woicik PA, Wang R, Telang F, Volkow ND (2009b) Dopaminergic Response to Drug Words in Cocaine Addiction. J Neurosci 29:6001–6006.

Goldstein RZ, Tomasi D, Rajaram S, Cottone LA, Zhang L, Maloney T, Telang F, Alia-Klein N, Volkow ND (2007) Role of the anterior cingulate and medial orbitofrontal cortex in processing drug cues in cocaine addiction. Neuroscience 144:1153–1159.

Goldstein RZ, Volkow ND (2002) Drug addiction and its underlying neurobiological basis: neuroimaging evidence for the involvement of the frontal cortex. Am J Psychiatry 159:1642–1652.

Goldstein RZ, Volkow ND (2011) Dysfunction of the prefrontal cortex in addiction: neuroimaging findings and clinical implications. Nat Rev Neurosci 12:652–669.

Gorgolewski K, Burns CD, Madison C, Clark D, Halchenko YO, Waskom ML, Ghosh SS (2011) Nipype: A Flexible, Lightweight and Extensible Neuroimaging Data Processing Framework in Python. Front Neuroinform 5 Available at: https://www.frontiersin.org/articles/10.3389/fninf.2011.00013/full [Accessed September 20, 2019].

Gorgolewski KJ et al. (2016) The brain imaging data structure, a format for organizing and describing outputs of neuroimaging experiments. Sci Data 3:1–9.

Gossop M, Griffiths P, Powis B, Strang J (1992) Severity of dependence and route of administration of heroin, cocaine and amphetamines. Br J Addict 87:1527–1536.

Greve DN, Fischl B (2009) Accurate and robust brain image alignment using boundary-based registration. NeuroImage 48:63–72.

Harlé KM, Yu AJ, Paulus MP (2019) Bayesian computational markers of relapse in methamphetamine dependence. NeuroImage: Clinical 22:101794.

Harlé KM, Zhang S, Ma N, Yu AJ, Paulus MP (2016) Reduced Neural Recruitment for Bayesian Adjustment of Inhibitory Control in Methamphetamine Dependence. Biol Psychiatry Cogn Neurosci Neuroimaging 1:448–459.

Hayashi T, Ko JH, Strafella AP, Dagher A (2013) Dorsolateral prefrontal and orbitofrontal cortex interactions during self-control of cigarette craving. Proc Natl Acad Sci U S A 110:4422–4427.

Herbert C, Sütterlin S (2011) Response Inhibition and Memory Retrieval of Emotional Target Words: Evidence from an Emotional Stop-Signal Task. Journal of Behavioral and Brain Science 1:153–159.

Hester R, Dixon V, Garavan H (2006) A consistent attentional bias for drug-related material in active cocaine users across word and picture versions of the emotional Stroop task. Drug and Alcohol Dependence 81:251–257.

Hester R, Garavan H (2004) Executive dysfunction in cocaine addiction: evidence for discordant frontal, cingulate, and cerebellar activity. J Neurosci 24:11017–11022.

Ho D, Imai K, King G, Stuart EA (2011) MatchIt: Nonparametric Preprocessing for Parametric Causal Inference. Journal of Statistical Software 42:1–28.

Hu S, Ide JS, Zhang S, Sinha R, Li CR (2015) Conflict anticipation in alcohol dependence — A model-based fMRI study of stop signal task. NeuroImage: Clinical 8:39–50.

Jenkinson M, Bannister P, Brady M, Smith S (2002) Improved optimization for the robust and accurate linear registration and motion correction of brain images. Neuroimage 17:825–841.

Jensen AR, Rohwer WD (1966) The stroop color-word test: A review. Acta Psychologica 25:36–93.

Kalanthroff E, Cohen N, Henik A (2013) Stop feeling: inhibition of emotional interference following stop-signal trials. Front Hum Neurosci 7 Available at: https://www.frontiersin.org/articles/10.3389/fnhum.2013.00078/full [Accessed February 6, 2021].

Kampman KM, Volpicelli JR, McGinnis DE, Alterman AI, Weinrieb RM, D'Angelo L, Epperson LE (1998) Reliability and validity of the Cocaine Selective Severity Assessment. Addict Behav 23:449–461.

Kober H, Lacadie CM, Wexler BE, Malison RT, Sinha R, Potenza MN (2016) Brain Activity During Cocaine Craving and Gambling Urges: An fMRI Study. Neuropsychopharmacology 41:628–637.

Konova AB, Parvaz MA, Bernstein V, Zilverstand A, Moeller SJ, Delgado MR, Alia-Klein N, Goldstein RZ (2019) Neural mechanisms of extinguishing drug and pleasant cue associations in human addiction: role of the VMPFC. Addiction Biology 24:88–99.

Lee H-H, Hsieh S (2017) Resting-State fMRI Associated with Stop-Signal Task Performance in Healthy Middle-Aged and Elderly People. Front Psychol 8 Available at: https://www.ncbi.nlm.nih.gov/pmc/articles/PMC5427072/ [Accessed February 13, 2021].

Li CR, Huang C, Constable RT, Sinha R (2006a) Imaging Response Inhibition in a Stop-Signal Task: Neural Correlates Independent of Signal Monitoring and Post-Response Processing. J Neurosci 26:186–192.

Li CR, Huang C, Yan P, Bhagwagar Z, Milivojevic V, Sinha R (2008) Neural Correlates of Impulse Control During Stop Signal Inhibition in Cocaine-Dependent Men. Neuropsychopharmacology 33:1798–1806.

Li CR, Milivojevic V, Kemp K, Hong K, Sinha R (2006b) Performance monitoring and stop signal inhibition in abstinent patients with cocaine dependence. Drug and Alcohol Dependence 85:205–212.

Li C-SR, Luo X, Yan P, Bergquist K, Sinha R (2009) Altered impulse control in alcohol dependence: neural measures of stop signal performance. Alcohol Clin Exp Res 33:740–750.

Li X, Morgan PS, Ashburner J, Smith J, Rorden C (2016) The first step for neuroimaging data analysis: DICOM to NIfTI conversion. J Neurosci Methods 264:47–56.

Logan G, Cowan W (1984) On the ability to inhibit thought and action: A theory of an act of control. Psychological Review 91:295–327.

Martinez D, Slifstein M, Narendran R, Foltin RW, Broft A, Hwang D-R, Perez A, Abi-Dargham A, Fischman MW, Kleber HD, Laruelle M (2009) Dopamine D1 Receptors in Cocaine Dependence Measured with PET and the Choice to Self-Administer Cocaine. Neuropsychopharmacol 34:1774–1782.

Matuskey D, Luo X, Zhang S, Morgan PT, Abdelghany O, Malison RT, Li CR (2013) Methylphenidate remediates error-preceding activation of the default mode brain regions in cocaine-addicted individuals. Psychiatry Research: Neuroimaging 214:116–121.

McLellan AT, Kushner H, Metzger D, Peters R, Smith I, Grissom G, Pettinati H, Argeriou M (1992) The Fifth Edition of the Addiction Severity Index. J Subst Abuse Treat 9:199–213.

Moeller SJ, Maloney T, Parvaz MA, Alia-Klein N, Woicik PA, Telang F, Wang G-J, Volkow ND, Goldstein RZ (2010) Impaired insight in cocaine addiction: laboratory evidence and effects on cocaine-seeking behaviour. Brain 133:1484–1493.

Moeller SJ, Maloney T, Parvaz MA, Dunning JP, Alia-Klein N, Woicik PA, Hajcak G, Telang F, Wang G-J, Volkow ND, Goldstein RZ (2009) Enhanced choice for viewing cocaine pictures in cocaine addiction. Biol Psychiatry 66:169–176.

Moeller SJ, Zilverstand A, Konova AB, Kundu P, Parvaz MA, Preston-Campbell R, Bachi K, Alia-Klein N, Goldstein RZ (2018) Neural correlates of drug-biased choice in currently-using and abstinent individuals with cocaine use disorder. Biol Psychiatry Cogn Neurosci Neuroimaging 3:485–494.

Parvaz MA, Konova AB, Proudfit GH, Dunning JP, Malaker P, Moeller SJ, Maloney T, Alia-Klein N, Goldstein RZ (2015) Impaired Neural Response to Negative Prediction Errors in Cocaine Addiction. J Neurosci 35:1872–1879.

Parvaz MA, Maloney T, Moeller SJ, Woicik PA, Alia-Klein N, Telang F, Wang G-J, Squires NK, Volkow ND, Goldstein RZ (2012) Sensitivity to monetary reward is most severely compromised in recently abstaining cocaine addicted individuals: A cross-sectional ERP study. Psychiatry Research: Neuroimaging 203:75–82.

Phillips PEM, Stuber GD, Heien MLAV, Wightman RM, Carelli RM (2003) Subsecond dopamine release promotes cocaine seeking. Nature 422:614–618.

Raichle ME, MacLeod AM, Snyder AZ, Powers WJ, Gusnard DA, Shulman GL (2001) A default mode of brain function. Proc Natl Acad Sci U S A 98:676–682.

Raud L, Westerhausen R, Dooley N, Huster RJ (2020) Differences in unity: The go/no-go and stop signal tasks rely on different mechanisms. NeuroImage 210:116582.

Ray S, Haney M, Hanson C, Biswal B, Hanson SJ (2015) Modeling Causal Relationship Between Brain Regions Within the Drug-Cue Processing Network in Chronic Cocaine Smokers. Neuropsychopharmacology 40:2960–2968.

Sakoglu U, Mete M, Esquivel J, Rubia K, Briggs R, Adinoff B (2019) Classification of cocaine-dependent participants with dynamic functional connectivity from functional magnetic resonance imaging data. J Neurosci Res 97:790–803.

Sjoerds Z, Brink W van den, Beekman ATF, Penninx BWJH, Veltman DJ (2014) Response inhibition in alcohol-dependent patients and patients with depression/anxiety: a functional magnetic resonance imaging study. Psychological Medicine 44:1713–1725.

Smith DG, Ersche KD (2014) Using a drug-word Stroop task to differentiate recreational from dependent drug use. CNS Spectr 19:247–255.

Tiffany ST, Singleton E, Haertzen CA, Henningfield JE (1993) The development of a cocaine craving questionnaire. Drug Alcohol Depend 34:19–28.

Tustison NJ, Avants BB, Cook PA, Zheng Y, Egan A, Yushkevich PA, Gee JC (2010) N4ITK: Improved N3 Bias Correction. IEEE Transactions on Medical Imaging 29:1310–1320.

Utevsky AV, Smith DV, Huettel SA (2014) Precuneus Is a Functional Core of the Default-Mode Network. J Neurosci 34:932–940.

Verbruggen F et al. (2019) A consensus guide to capturing the ability to inhibit actions and impulsive behaviors in the stop-signal task Frank MJ, Badre D, Egner T, Swick D, eds. eLife 8:e46323.

Verbruggen F, Houwer JD (2007) Do emotional stimuli interfere with response inhibition? Evidence from the stop signal paradigm. Cognition and Emotion 21:391–403.

Verbruggen F, Logan GD (2008) Response inhibition in the stop-signal paradigm. Trends Cogn Sci (Regul Ed) 12:418–424.

Vonmoos M, Hulka LM, Preller KH, Jenni D, Schulz C, Baumgartner MR, Quednow BB (2013) Differences in self-reported and behavioral measures of impulsivity in recreational and dependent cocaine users. Drug and Alcohol Dependence 133:61–70.

Wager TD, Nichols TE (2003) Optimization of experimental design in fMRI: a general framework using a genetic algorithm. Neuroimage 18:293–309.

Wang W, Worhunsky PD, Zhang S, Le TM, Potenza MN, Li C-SR (2018) Response inhibition and fronto-striatal-thalamic circuit dysfunction in cocaine addiction. Drug Alcohol Depend 192:137–145.

Woicik PA, Moeller SJ, Alia-Klein N, Maloney T, Lukasik TM, Yeliosof O, Wang G-J, Volkow ND, Goldstein RZ (2009) The neuropsychology of cocaine addiction: recent cocaine use masks impairment. Neuropsychopharmacology 34:1112–1122.

Woolrich MW, Ripley BD, Brady M, Smith SM (2001) Temporal Autocorrelation in Univariate Linear Modeling of FMRI Data. NeuroImage 14:1370–1386.

Zhang Y, Brady M, Smith S (2001) Segmentation of brain MR images through a hidden Markov random field model and the expectation-maximization algorithm. IEEE Transactions on Medical Imaging 20:45–57.

Zhang Y, Zhang S, Ide JS, Hu S, Zhornitsky S, Wang W, Dong G, Tang X, Li C-SR (2018) Dynamic network dysfunction in cocaine dependence: Graph theoretical metrics and stop signal reaction time. Neuroimage Clin 18:793–801.

Zhao R, Zhang X, Fei N, Zhu Y, Sun J, Liu P, Yang X, Qin W (2019) Decreased cortical and subcortical response to inhibition control after sleep deprivation. Brain Imaging Behav 13:638–650.

Zhukovsky P, Morein-Zamir S, Ziauddeen H, Fernandez-Egea E, Meng C, Regenthal R, Sahakian BJ, Bullmore ET, Robbins TW, Dalley JW, Ersche KD (2021) Prefrontal cortex activation and stopping performance underlie the beneficial effects of atomoxetine on response inhibition in healthy and cocaine use disorder volunteers. Biological Psychiatry: Cognitive Neuroscience and Neuroimaging Available at: https://www.sciencedirect.com/science/article/pii/S2451902221002524 [Accessed September 14, 2021].

Zilverstand A, Huang AS, Alia-Klein N, Goldstein RZ (2018) Neuroimaging Impaired Response Inhibition and Salience Attribution in Human Drug Addiction: A Systematic Review. Neuron 98:886–903.

Figure legends

Figure 1. The Emotional Stop-Signal Task. Participants are instructed to respond via button presses as quickly and accurately as possible to the change in word color from white to blue/green, and to suppress their responses when the word color turns red after a variable delay (i.e., the stop-signal delay, or SSD). Uniquely, word categories comprised neutral words, as well as drug, food, and threat-related words, permitting the examination of emotional reactivity during inhibitory control. Typical SST figure adapted from Aron and Poldrack, 2006.

Figure 2. CUD and HC groups' SSRT in response to each cue type. We found no significant main effects of Group or Cue but found a significant Group x Cue interaction ($p = .027$), where HC were significantly slower to stop than the CUD group in response to Food and Neutral cues. No drug-cue-related group differences were evident in SSRT.

Figure 3. Brain activity differences across CUD and HC groups during inhibitory control, regardless of cue type. The analysis of overall inhibitory control revealed significantly lower activity in the left dmPFC in the CUD group compared to HC. Cluster defining threshold: $Z > 3.1$ ($p < .001$), cluster corrected at $p < .05$. The bar plot of activation patterns shows relative activation to all cue types within the voxels that display peak activation as a result of the overall inhibitory control contrast. Inhibitory control was modeled via the hallmark Stop_Success > Stop_Fail contrast of task events corresponding to all cues.

Figure 4. Brain activity differences across CUD and HC groups during inhibitory control under drug cue reactivity. The linear contrast of drug cue- versus a competing, non-drug positive reinforcer, food cue-related inhibitory control revealed significantly lower activity in the left dlPFC in the CUD group compared to HC. Cluster defining threshold: $Z > 3.1$ ($p < .001$), cluster corrected at $p < .05$. The bar plot of activation patterns shows relative activation to all cue types within the voxels that display peak

activation as a result of the Drug > Food inhibitory control contrast. Inhibitory control was modeled via the hallmark Stop_Success > Stop_Fail contrast of task events corresponding to drug and food cues.

Figure 5. Whole-brain correlational analysis of cocaine use severity as assayed by recent cocaine use frequency in the past month, and its relationship with inhibitory control under drug cue reactivity (Drug > Food inhibitory control contrast). When entered into the GLM as a covariate in a whole-brain analysis, recent cocaine use frequency showed significant positive correlations with activity in the right OFC, right dmPFC, and left dlPFC in the CUD group, such that the more severe the cocaine use, the higher the activation in these prefrontal regions during inhibitory control under drug cue reactivity. Cluster defining threshold: $Z > 3.1$ ($p < .001$), cluster corrected at $p < .05$. Inhibitory control was modeled via the hallmark Stop_Success > Stop_Fail contrast of task events corresponding to drug and food cues.

Typical stop-signal task

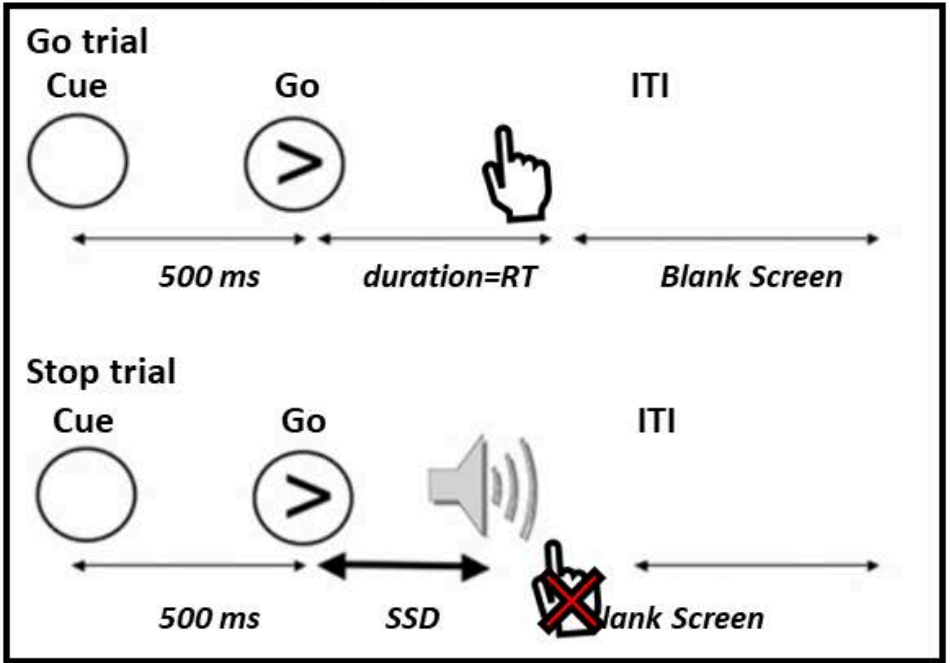

Emotional stop-signal task

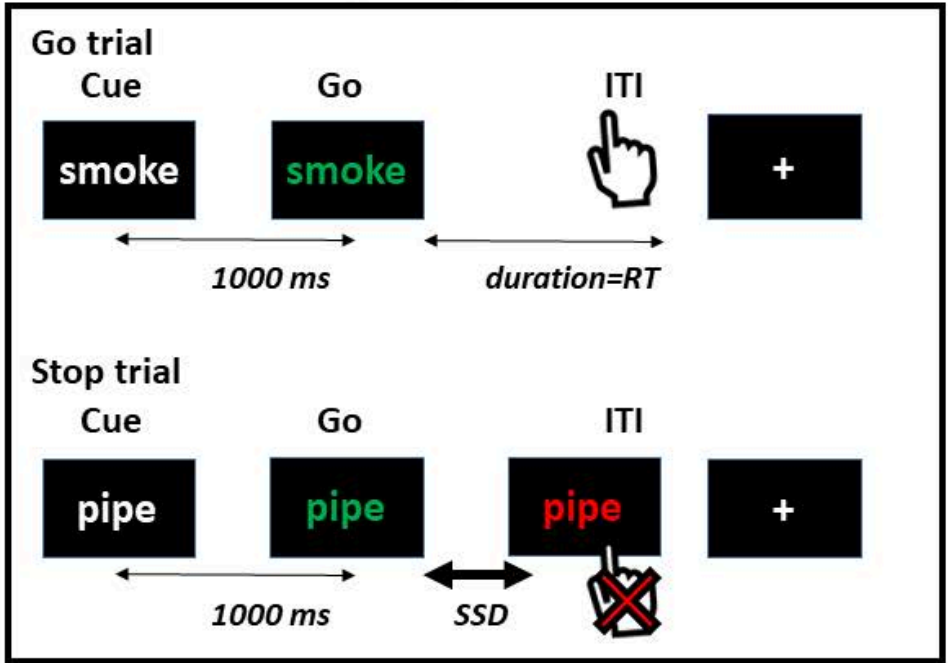

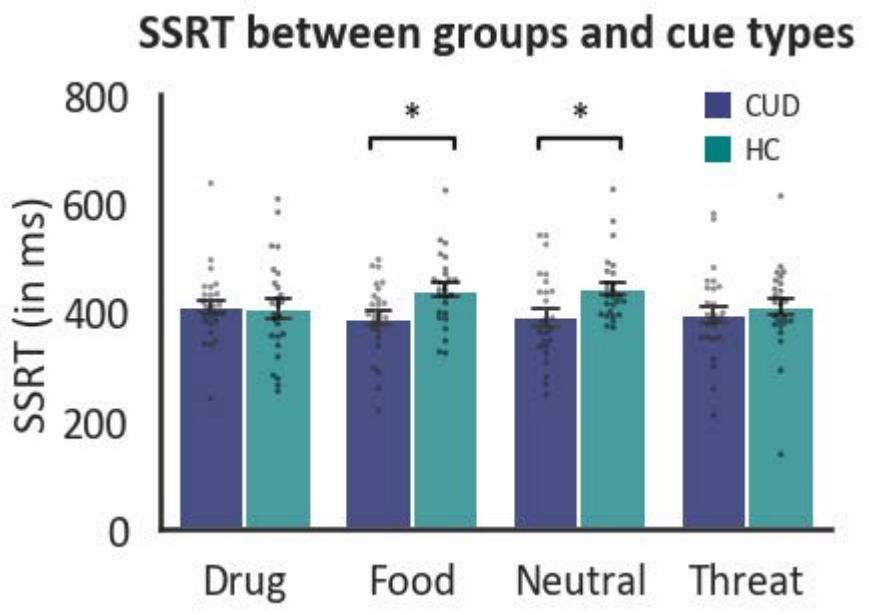
SSRT between groups and cue types
800
600
400
200
0
SSRT (in ms)
*
*
CUD
HC
Drug
Food
Neutral
Threat

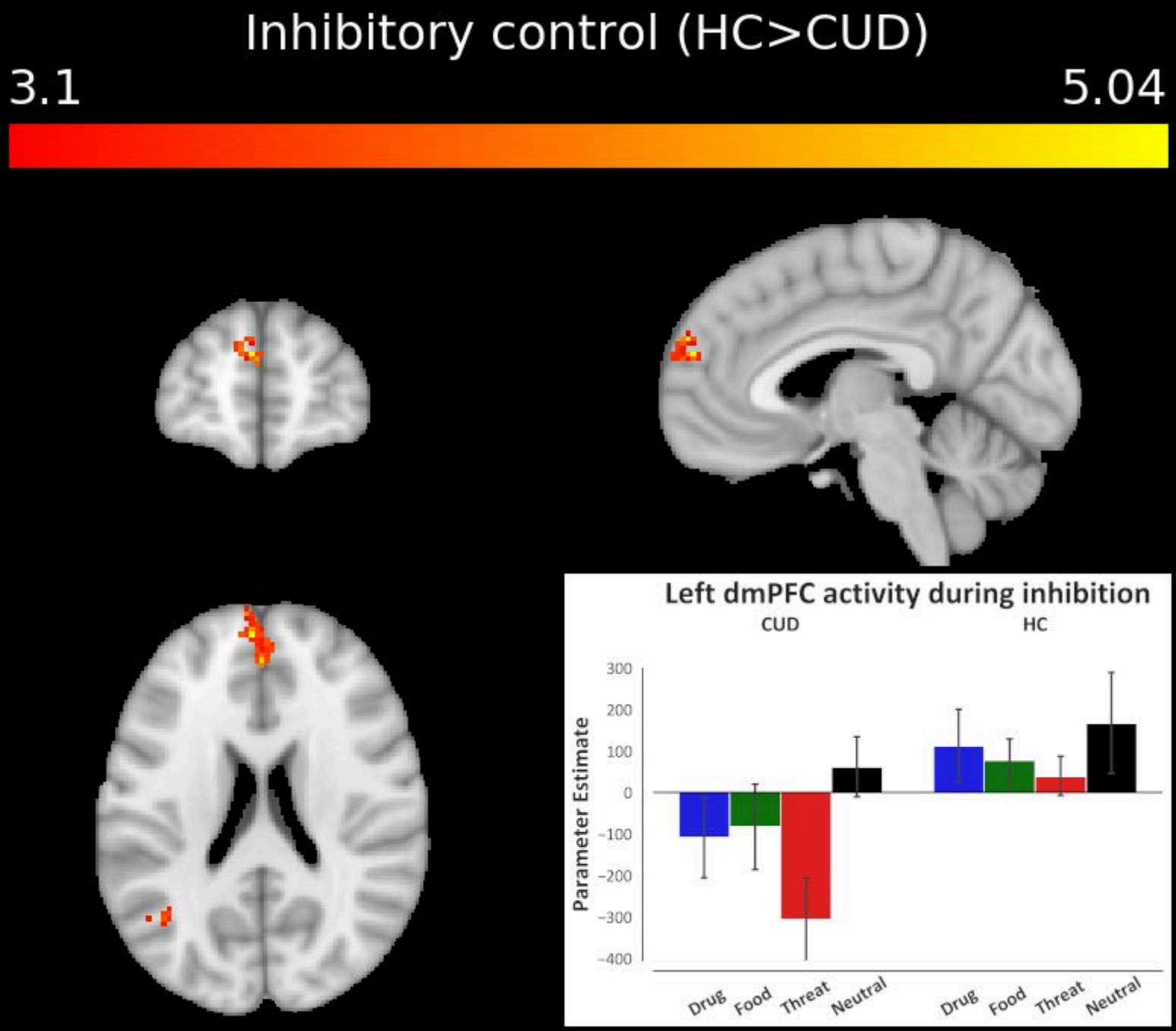
Inhibitory control (HC>CUD)
3.1
5.04
Left dmPFC activity during inhibition
CUD
HC
Parameter Estimate
300
200
100
0
-100
-200
-300
-400
Drug
Food
Threat
Neutral
Drug
Food
Threat
Neutral

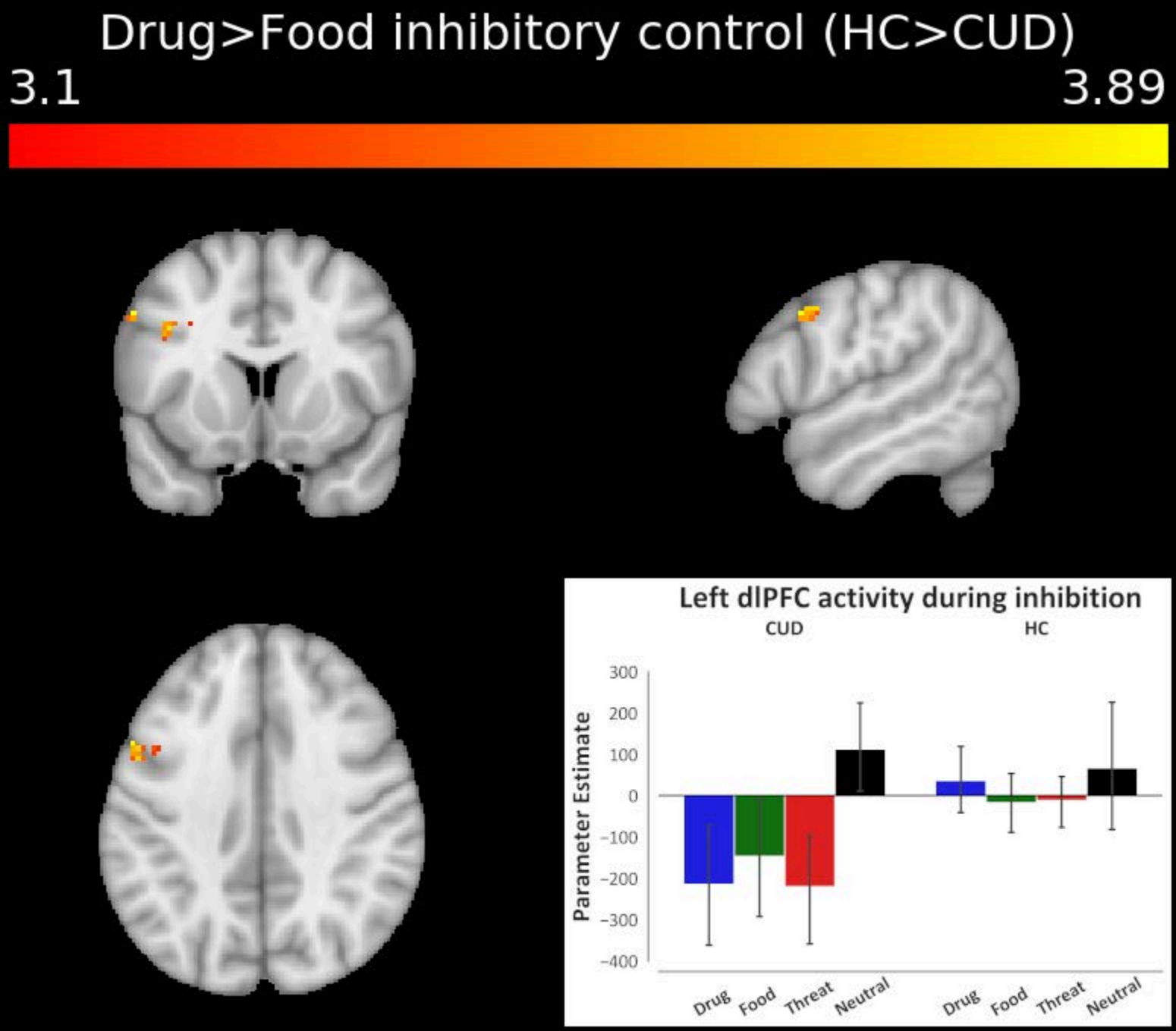
Drug>Food inhibitory control (HC>CUD)
3.1
3.89
Left dlPFC activity during inhibition
CUD
HC
Parameter Estimate
300
200
100
0
-100
-200
-300
-400
Drug
Food
Threat
Neutral
Drug
Food
Threat
Neutral

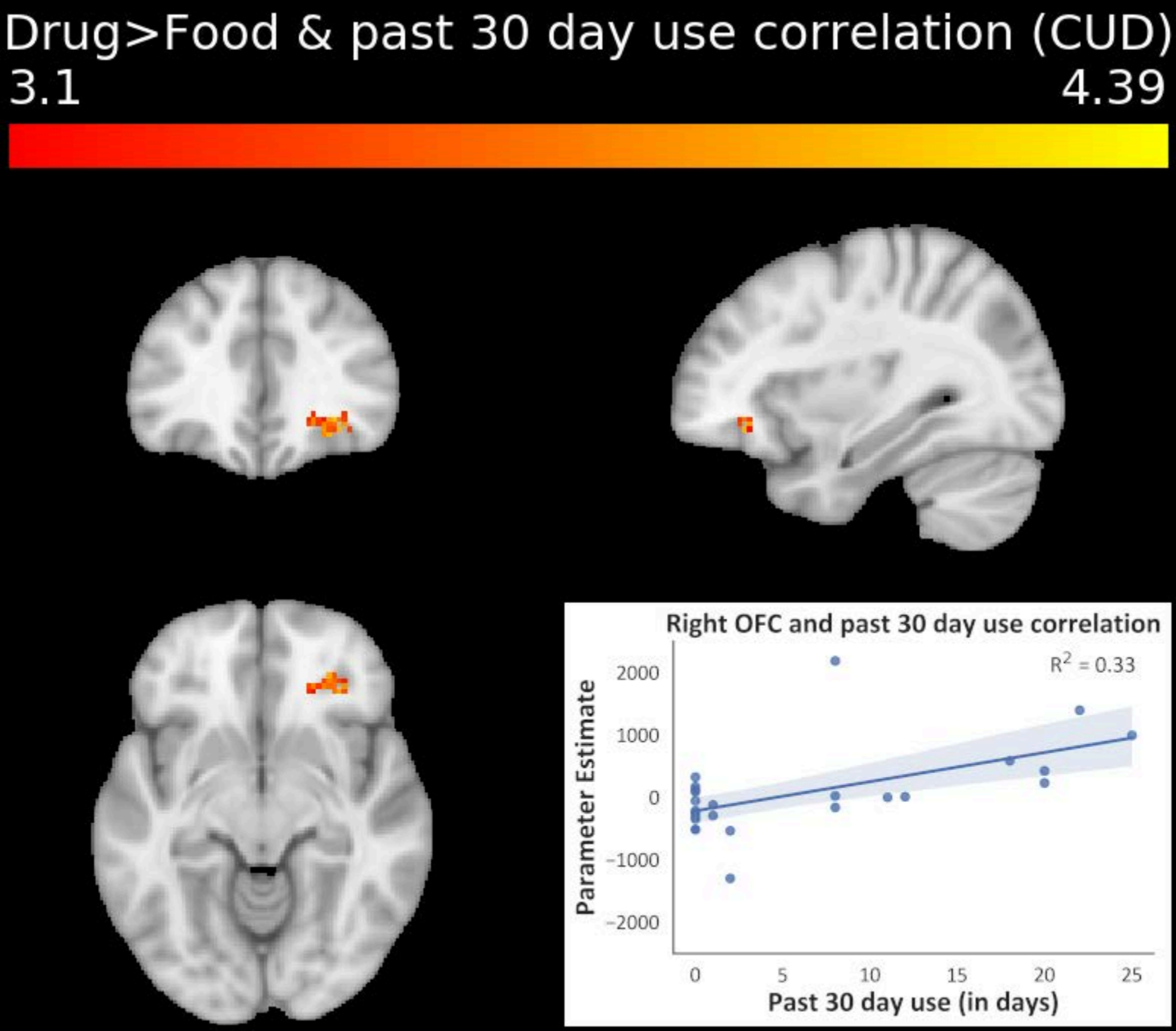
Drug>Food & past 30 day use correlation (CUD)
3.1
4.39
Right OFC and past 30 day use correlation
R^2 = 0.33
Parameter Estimate
2000
1000
0
−1000
−2000
0
5
10
15
20
25
Past 30 day use (in days)

Table 1. Sample profile.

	CUD (n = 26)	**HC (n = 26)**	**Significance test**
Age	44.07 ± 8.18 Min: 28, Max: 59	42.66 ± 7.05 Min: 27, Max: 55	$t(50) = 0.67$, $p = .509$
Sex (M/F)	22/4	21/5	$\chi2(1) = 0.13$, $p = .718$
Race (Black/White/Other/Unreported)	17/3/4/2	16/4/6/0	$\chi2(2) = 1.69$, $p = .430$
Education (years; 12=high school grad)	12.27 ± 1.59 Min: 9, Max: 16	12.92 ± 1.72 Min: 10, Max: 16	$t(50) = 1.42$, $p = .160$
Verbal IQ (std. WRAT-III score)	95.04 ± 11.65 Min: 76, Max: 116	99.00 ± 11.30 Min: 75, Max: 113	$t(50)= 1.24$, $p = .219$
Non-verbal IQ (matrix reasoning score)	8.96 ± 2.99 Min: 3, Max: 14	11.12 ± 2.16 Min: 4, Max: 15	$t(50) = 2.98$, $p = .004$*
Cigarette use per day (cigarettes)	5.11 ± 6.20 Min: 0, Max: 25	2.92 ± 6.21 Min: 0, Max: 20	$t(50) = 1.27$, $p = .209$
Depression (BDI score)	7.81 ± 7.65 Min: 0, Max: 24	4.46 ± 5.69 Min: 0, Max: 20	$t(50) = 1.79$, $p = .079$
Duration of cocaine use (years)	16.00 ± 8.15 Min: 3, Max: 30	--	--
Past month cocaine use (days/month)	6.08 ± 8.34 Min: 0, Max: 25	--	--
Days since last cocaine use	293.23 ± 530.65 Min: 0, Max: 1825	--	--
Cocaine Severity of Dependence Scale	5.04 ± 4.87 Min: 0, Max: 15	--	--
Cocaine Selective Severity Assessment	16.35 ± 11.33 Min: 0, Max: 37	--	--

Cocaine Craving Questionnaire	13.73 ± 13.78 Min: 0, Max: 45	--	--

Note: Significant group differences are flagged with an asterisk. ± denotes standard deviation.

Table 2. Behavioral inhibitory control performance.

		CUD (n = 26)	HC (n = 26)	Significance test [b]
Average [a]				
	Go RT	802.48 ± 73.39	777.66 ± 59.03	$t(50) = 1.34$, $p = .185$
		Min: 641.51, Max: 909.12	Min: 640.56, Max: 860.80	
	SSRT	396.07 ± 52.02	423.66 ± 60.14	$t(50) = 1.77$, $p = .083$
		Min: 312.25, Max: 556.25	Min: 280.25, Max: 616.64	
	Go %	77.79 ± 9.48	84.17 ± 11.35	$t(50) = 2.20$, $p = .032$
		Min: 62.5, Max: 98.96	Min: 62.5, Max: 100	
	Stop %	53.43 ± 9.04	56.65 ± 9.10	$t(50) = 1.28$, $p = .207$
		Min: 25.00, Max: 70.83	Min: 37.14, Max: 72.09	
Drug				
	Go RT	805.75 ± 80.93	773.47 ± 61.81	$t(50) = 1.62$, $p = .112$
		Min: 640.54, Max: 931.86	Min: 619.23, Max: 860.12	
	SSRT	409.60 ± 68.37	404.83 ± 91.19	$t(50) = 0.21$, $p = .832$
		Min: 241.00, Max: 636.00	Min: 254.00, Max: 606.89	
	Go %	77.58 ± 12.07	84.41 ± 11.85	$t(50) = 2.06$, $p = .045$
		Min: 54.17, Max: 100.00	Min: 62.5, Max: 100	
	Stop %	52.35 ± 10.91	58.45 ± 12.86	$t(50) = 1.85$, $p = .071$
		Min: 16.67, Max: 66.67	Min: 27.87, Max: 83.33	
Food				
	Go RT	799.42 ± 70.55	779.67 ± 66.90	$t(50) = 1.03$, $p = .305$
		Min: 655.71, Max: 908.67	Min: 638.64, Max: 874.24	
	SSRT	388.83 ± 67.55	439.81 ± 66.62	$t(50) = 2.74$, $p = .008$*
		Min: 219.00, Max: 495.67	Min: 323.78, Max: 622.67	
	Go %	78.84 ± 11.35	83.98 ± 13.96	$t(50) = 1.46$, $p = .151$

		Min: 55.56, Max: 100.00	Min: 50.00, Max: 100.00	
	Stop %	54.38 ± 11.23	55.50 ± 9.52	$t(50) = 0.39$, $p = .699$
		Min: 33.33, Max: 83.33	Min: 33.33, Max: 80.00	
Threat				
	Go RT	804.35 ± 83.30	775.37 ± 57.58	$t(50) = 1.46$, $p = .151$
		Min: 626.92, Max: 925.00	Min: 656.21, Max: 880.30	
	SSRT	395.82 ± 81.20	408.28 ± 80.87	$t(50) = 0.55$, $p = .582$
		Min: 209.44, Max: 580.00	Min: 137.78, Max: 612.44	
	Go %	76.34 ± 11.66	83.79 ± 12.63	$t(50) = 2.21$, $p = .031$
		Min: 50.00, Max: 100.00	Min: 58.33, Max: 100.00	
	Stop %	52.62 ± 12.32	57.67 ± 9.23	$t(50) = 1.67$, $p = .101$
		Min: 16.67, Max: 83.33	Min: 44.44, Max: 83.33	
Neutral				
	Go RT	802.18 ± 69.55	783.41 ± 60.69	$t(50) = 1.04$, $p = .305$
		Min: 642.83, Max: 905.67	Min: 647.83, Max: 870.04	
	SSRT	390.03 ± 79.38	441.70 ± 60.76	$t(50) = 2.64$, $p = .011$*
		Min: 247.83, Max: 540.22	Min: 371.00, Max: 624.56	
	Go Accuracy %	78.42 ± 13.08	84.48 ± 13.60	$t(50) = 1.64$, $p = .101$
		Min: 55.56, Max: 100.00	Min: 50.00, Max: 100.00	
	Stop Accuracy %	54.38 ± 9.13	56.08 ± 9.08	$t(50) = 0.67$, $p = .503$
		Min: 33.33, Max: 83.33	Min: 33.33, Max: 72.73	

Note: All RT values in milliseconds. ± denotes standard deviation. [a] Average (i.e., collapsed across all cue types) accuracy and RT values were used for inclusion criteria to abide by the horse-race model assumptions of the stop-signal task (i.e., positive SSRT, Go Accuracy ≥ 60%, Stop Accuracy between 25-75%). [b] Significance tests reflect independent samples t-tests for each variable between groups. Because only the SSRT variable was of interest (and yielded a significant Group x Cue interaction), no other RT or accuracy variables are flagged with asterisks when $p < .05$.

Table 3. Inhibitory control related BOLD signal, all participants

	Side	Voxels	Peak Z	x	y	z	BA
Overall inhibitory control related BOLD signal (all cues)							
Medial Frontal Cortex	R	271	5.17	1	50	-13	BA10
Frontal Pole	L	209	5.12	-19	46	44	BA8
Orbitofrontal Cortex	L	75	4.61	-27	33	-13	BA47
Superior Frontal Gyrus	R	121	4.59	26	29	54	BA8
Inferior Frontal Gyrus	L	51	4.02	-51	29	10	BA45
Subcallosal Cortex	R	265	5.41	5	5	-13	--
Anterior Superior Temporal Gyrus	R	336	5.1	59	-5	-13	BA22
Middle Temporal Gyrus	L	181	5.12	-53	-8	-17	BA21
Anterior Parahippocampal Gyrus	R	95	4.49	22	-16	-19	--
Posterior Superior Temporal Gyrus	L	54	4.17	-66	-25	2	BA22
Posterior Superior Temporal Gyrus	R	148	4.49	54	-35	6	BA22
Precuneus	L	384	4.88	-4	-57	17	BA23
Superior Lateral Occipital Cortex	R	209	4.69	52	-66	29	BA39
Superior Lateral Occipital Cortex	L	231	4.68	-45	-76	40	BA39
Superior Lateral Occipital Cortex	R	53	4.41	26	-78	46	BA7
Superior Lateral Occipital Cortex	R	59	4.28	22	-83	17	BA19
Occipital Pole	L	71	4.19	-15	-98	14	V2
Correlation of mean SSRT and overall inhibitory control related BOLD signal (all cues)							
Frontal Pole	R	58	4.54	29	59	8	BA10
Paracingulate Gyrus	R	52	4.47	7	42	27	BA9
Middle Frontal Gyrus	R	106	4.51	33	29	31	BA9
Middle Frontal Gyrus	R	99	4.24	41	16	50	BA8
Middle Frontal Gyrus	L	85	4.38	-36	16	40	BA8
Thalamus	R	323	5.46	5	-14	8	--

Putamen	L	51	4.17	-27	-27	0	--
Posterior Cingulate Gyrus	R	135	5.08	3	-40	25	BA23
Posterior Supramarginal Gyrus	R	108	4.24	52	-44	46	BA40
Superior Lateral Occipital Cortex	L	92	4.65	-45	-61	46	BA39
Precuneus	R	58	4.83	7	-70	40	BA7
Occipital Pole	R	147	5.48	24	-100	0	V2

Note: Inhibitory control related BOLD signal derived by the hallmark Stop_Success > Stop_Fail contrast.

Table 4. Whole-brain Drug > Food and Drug > Neutral inhibitory control related BOLD signal correlations with drug use measures, CUD group only

	Side	Voxels	Peak Z	x	y	z	BA
Drug > Food inhibitory control related BOLD signal							
Past 30-day cocaine use							
Orbitofrontal Cortex	R	99	4.39	33	35	-9	BA47
Superior Frontal Gyrus	R	69	4.15	20	25	54	BA6
Middle Frontal Gyrus	L	133	4.27	-40	5	50	BA6
Cocaine craving							
Middle Frontal Gyrus	R	61	4.32	46	44	25	*BA9*
Inferior Frontal Gyrus	R	71	4.2	44	14	25	BA44
Middle Temporal Gyrus	R	153	4.54	52	-5	-21	BA21
Length of abstinence							
Frontal Pole	R	59	-4.25	29	53	12	BA10
Middle Frontal Gyrus	R	109	-4.17	48	14	35	BA44
Precentral Gyrus	R	163	-4.42	35	-5	67	BA6
Drug > Neutral inhibitory control related BOLD signal							
Past 30-day cocaine use							
Middle Frontal Gyrus	L	66	4.16	-42	14	46	BA8
Cocaine craving							
Frontal Pole	L	53	4.17	-19	48	48	BA8
Middle Frontal Gyrus	L	68	5.11	-42	38	27	BA10
Superior Frontal Gyrus	R	90	4.35	3	23	63	BA6
Inferior Frontal Gyrus	L	88	4.82	-53	23	25	BA44
Hippocampus	R	55	4.21	22	-20	-13	--
Length of abstinence							

No significant clusters

Note: Inhibitory control related BOLD signal derived by the hallmark Stop_Success > Stop_Fail contrast.